

Inner-Sphere Complexation of Cobalt(II) 2,9-Dimethyl-1,10-phenanthroline ([Co(neo)]²⁺) with Commercial and Sol–Gel Derived Silica Gel Surfaces

Colleen M. Taylor,[†] Stephen P. Watton,^{*†} Peter A. Bryngelson,[‡] and Michael J. Maroney[‡]

Department of Chemistry, Virginia Commonwealth University, 1001 West Main Street, Richmond, Virginia 23284, and Department of Chemistry, University of Massachusetts, 701 Lederle Graduate Research Tower, 710 North Pleasant Street, Amherst, Massachusetts 01003-9336

Received June 26, 2002

[Co(2,9-dimethyl-1,10-phenanthroline)(solvent)₄]²⁺ ([Co(neo)]²⁺) undergoes a significant decrease in symmetry to form an inner-sphere surface complex when grafted directly on preformed silica or introduced during the sol–gel process. The visible and X-ray absorption spectra of the surface adducts are interpreted in terms of a binding mode in which the Co(II) center has a highly distorted pseudo-*C*_{2v} symmetry. The interaction of [Co(neo)]²⁺ with the silica surface was analyzed using an acid–base equilibrium relationship. Half-maximal surface binding was observed at pH ca. 6. Linear fits to the pH dependence data are consistent with inner-sphere binding of a single silanol group to the cobalt center. The formation of the surface species in tetramethoxyorthosilicate (TMOS) sol–gels required approximately 2 equiv of hydroxide anion per cobalt center, suggesting a two-proton-dependent binding event to form a species such as [Co(neo)(SiO)₂]. Both sol–gel and silica samples showed essentially identical visible and X-ray absorption spectra, indicating formation of very similar surface adducts when the different synthesis procedures were employed. The maximal binding of [Co(neo)]²⁺ on three silica samples with different pore diameters and surface areas was compared. Increased binding was found to be inversely proportional to surface area and proportional to pore diameter, indicating a preference for less sterically demanding surface sites.

Introduction

The application of coordination chemistry principles to the understanding of silica and other oxide materials as ligands originated in the 1960s, when it was initially demonstrated that oxide surface groups can act as inner-sphere ligands,^{1–3} and has developed into a focus area known as interfacial coordination chemistry (ICC).^{4,5} Research in this field aims to better understand the inner-sphere coordination chemistry that can occur between metal complexes and the surfaces of oxide supports such as silica, with the ultimate objective of

improving the rational design of supported catalyst systems. Of particular importance in engineering supported catalysts is evaluation of the homogeneity and specific identity of the active sites at the surface. These data are also essential if useful interpretation of mechanism is to be accomplished for surface-supported catalyst systems.

The studies described herein pertain to formation of a surface-coordinated adduct of cobalt neocuproine, [Co(neo)]²⁺, which is accompanied by a very uniform and pronounced change in coordination geometry at the metal center, from a six-coordinate pseudo-octahedral structure in solution to a four-coordinate pseudotetrahedral structure at the material surface. Our motivation to thoroughly characterize this particular surface compound was 2-fold. First, the significant change in spectroscopic behavior makes the species a good probe for surface structure and a good case study for ICC principles. Second, the materials show activity toward the disproportionation of hydrogen peroxide,⁶ and we were interested in understanding how this catalytic

* To whom correspondence should be addressed. E-mail: spwatton@mail1.vcu.edu.

[†] Virginia Commonwealth University.

[‡] University of Massachusetts.

- (1) Iler, R. K. *The Chemistry of Silica*; John Wiley & Sons: New York, 1979.
- (2) Burwell, R. L.; Pearson, R. G.; Haller, G. L.; Tjok, P. J.; Chock, S. P. *Inorg. Chem.* **1965**, *4*, 1123–1128.
- (3) Dugger, L. D.; Stanton, J. H.; Irby, B. N.; McConnell, B. L.; Cummings, W. W.; Maatman, R. W. *J. Phys. Chem.* **1964**, *68*, 757–310.
- (4) Lambert, J.-F.; Hoogland, M.; Che, M. *J. Phys. Chem. B.* **1997**, *101*, 10347–10355.
- (5) Lepetit, C.; Che, M. *J. Mol. Catal. A: Chem.* **1995**, *100*, 147–160.

(6) Taylor, C. M.; Watton, S. P. Unpublished results.

activity is related to the structural features of the surface-bound complex.

We report here our initial studies concerning the formation of the surface adduct, which include spectroscopic and pH-dependence data for the Co²⁺–silica interaction. On the basis of these data, we establish a number of important structural characteristics for the surface complex. In addition, we report results from a study comparing the interactions of the metal complex with the surfaces of different commercial silica gels, and with silica materials prepared in the presence of the metal complexes by sol–gel processing. The thorough characterization of the new surface adduct will aid in the study of the catalytic activity of this new complex, which will be described elsewhere.

Experimental Section

I. Chemicals and Instrumentation. Unless otherwise stated, all chemicals were of reagent grade and used as received from Aldrich. NaOH (1 M) solutions were prepared immediately before use, and concentrations were assayed by titration with standardized HCl, using phenolphthalein indicator. pH measurements were made using a Corning ion/pH analyzer 350 with gel filled electrode (VWR). UV–vis solution spectra were obtained on a Hewlett-Packard 8452A diode array spectrophotometer using 1 cm path-length polystyrene cuvettes. UV–vis measurements on opaque samples were made on the same instrument, employing a Labsphere RSA-HP-84 diffuse reflectance accessory. Solid samples for diffuse reflectance were diluted in KBr in an approximately 1:50 ratio and ground to an even and small particle size. KBr was used as a reflectivity reference. Diffuse reflectance measurements of grafted silica samples were taken without dilution in KBr. Spectra were obtained in transmittance mode and converted using the Kubelka–Munk function $[(1 - F_T)^2 / (2 \times F_T)]$ where F_T = fraction transmitted when collecting diffuse reflectance visible spectra.⁷ Mid-IR spectra were taken on a Nicolet Nexus 670 FT-IR equipped with an Avatar diffuse reflectance accessory, using Omnic software for data collection and analysis. The same instrument was used to obtain mid-IR data for [Co(neo)]²⁺ grafted on silica without the diffuse reflectance accessory. The sample was instead prepared in pellet form with KBr, and a KBr pellet with silica was used as background. Trial and error was required to obtain a background of appropriate intensity, and only peaks within the range 400–1700 cm⁻¹ were detectable because of intense absorptions from silica. All spectral data were processed using Kaleidagraph.⁸

II. X-ray Absorption Spectroscopy. XAS data for all samples were collected on beam line X9B at the National Synchrotron Light Source (NSLS) at Brookhaven National Laboratory. Data were collected using solid samples diluted with boron nitride. The samples were contained in polycarbonate holders that were inserted into slotted aluminum holders, covered with Kapton tape, and held near 50 K using a He displax cryostat for XAS data collection under dedicated conditions at 2.8 GeV and 160–260 mA as previously described.⁹ Data were collected using a Si(220) double crystal monochromator internally calibrated to the first inflection point of Co foil (7709.5 eV). The experimental arrangement provides a theoretical resolution of ca. 0.5 eV for the 0.5 mm hutch slit height

Table 1. XANES Analysis

cmpd	Co K-edge energy (eV)	1s → 3d peak area (×10 ² eV)
[Co(neo)(H ₂ O) ₄](NO ₃)	7718.4(1)	4.8(2)
[KCo(neo)(XDK)(PF ₆)]	7717.8(1)	15.7(2)
[Co(neo)(silica)] ⁿ⁺	7717.9(1)	11.8(4)
[Co(neo)(sol–gel)] ⁿ⁺	7718.3(1)	11.6(1)

employed. Harmonic rejection was accomplished with a focusing mirror left flat. X-ray fluorescence data were collected using a 13-element Ge detector (Canberra). Sample integrity during exposure to monochromatic synchrotron radiation was monitored by observing the Co K-edge spectrum on sequential scans. No changes in either the edge energy (redox state of Co) or XANES features (Co ligand environment) were observed.

The XAS spectra reported are the sum of duplicate scans, and the edge energy and X-ray absorption near edge structure (XANES) were analyzed in analogy with previously published procedures.⁹ For the purpose of comparison, the Co K-edge energy of the samples was taken to be the energy at a normalized absorbance of 0.5 (Table 1). The edge values are reproducible to ±0.1 eV. The areas under the peaks assigned to 1s → 3d transitions were determined by fitting a background to the region of the normalized spectrum immediately below and above this feature in energy and integrating the difference. Extended X-ray absorption fine structure (EXAFS) data were analyzed using the XAS analysis package WINXAS.¹⁰ Analysis of EXAFS features arising from atoms in the first coordination sphere was accomplished as previously described.¹¹

Theoretical phases and amplitudes for single scattering EXAFS analyses were obtained from FEFF 6^{12–14} calculations of the crystallographically characterized cation in the model compound, hexa-ammine-cobalt(III) tris(malonato-O,O′)-iron(III) pentahydrate,¹⁵ as previously described.¹¹

III. Surface Adsorption: Commercial Silica. A. General Synthesis. The formation of [Co(neo)(silica)]ⁿ⁺ was accomplished by addition of aqueous methanol solutions of a 1:1 mixture of [Co(NO₃)₂·6H₂O] (J. T. Baker) and neocuproine (GFS) to dry silica gel and equilibration in a constant-temperature water bath. All measurements for the equilibrium formation of the adsorbed species were taken after 24 h of incubation time. Loading of [Co(neo)]²⁺ on the surface, expressed as moles of [Co(neo)]²⁺ grafted per silicon, was estimated using a value of 40 wt % Si for silica brands Davisil 643, Merck 9385, and Merck 10181. The estimate for the percent Si was based on 40.43% found for Merck silica grade 9385 as determined by elemental analysis performed by Quantitative Technologies Inc. All surface areas given are as reported by the manufacturer.

B. Determination [Co²⁺] Bound to the Silica Surfaces. The concentration of adsorbed species was determined colorimetrically by combinations of solutions diluted appropriately with 15% NH₄SCN in acetone, maintaining at least a 75% vol/vol ratio of NH₄SCN/supernatant, a pH of the solution below 7, and an absorbance within a range 0.2–1 (hereafter, the thiocyanate test).¹⁶

(10) Ressler, T. J. *Physique IV* **1997**, 7, C2–269.

(11) Davidson, G.; Clugston, S. L.; Honek, J. F.; Maroney, M. J. *Inorg. Chem.* **2000**, 39, 2962–2963.

(12) Mustre de Leon, J.; Rehr, J. J.; Zabinsky, S. I.; Albers, R. C. *Phys. Rev.* **1991**, B44, 4146.

(13) Rehr, J. J.; Albers, R. C. *Phys. Rev.* **1990**, B41, 8139.

(14) Rehr, J. J.; Zabinsky, S. I.; Albers, R. C. *Phys. Rev. Lett.* **1992**, 69, 3397.

(15) Clegg, W. *Acta Crystallogr., Sect. C* **1985**, 41, 1164–1166.

(16) Sandell, E. B. *Colorimetric Determination of Traces of Metals*, 2nd ed.; Interscience Publishers: New York, 1950.

(7) Frodyma, M. M.; Lieu, V. T. In *Modern Aspects of Reflectance Spectroscopy*; Wendlandt, W. W., Ed.; Plenum Press: New York, 1968; Chapter 6.

(8) *Kaleidagraph*, 3.09 ed.; Synergy Software: Reading, PA, 1997.

(9) Bagyinka, C.; Whitehead, J. P.; Maroney, M. J. *J. Am. Chem. Soc.* **1993**, 115, 3576–3585.

A linear working curve for $[\text{Co}(\text{NCS})_4]^{2-}$ was established within this absorbance range ($\epsilon = 1841 \text{ M}^{-1} \text{ cm}^{-1}$ at 622 nm). Aliquots used in the analyses were obtained by one of two alternative methods, depending on the relative concentration of adsorbed species. Method 1: For low loadings (and hence high concentrations of Co^{2+} in the supernatant solutions), aliquots were drawn from the supernatant. Method 2: To obtain better sensitivity at high loadings (i.e., low Co^{2+} concentrations in the supernatant solutions), the samples were collected, rinsed with solutions having the same pH as the supernatant, dried, and then treated with a known volume of 0.1 M HCl to displace the Co^{2+} from the silica surface. Aliquots were then removed from the new supernatant for analysis. Independent measurements using both methods agreed within 5%.

C. pH Binding Curve. A 0.01 M stock solution of $[\text{Co}(\text{neo})]^{2+}$ was prepared from 0.291 g (1 mmol) of $[\text{Co}(\text{NO}_3)_2 \cdot 6\text{H}_2\text{O}]$ (J. T. Baker) and 0.21 g (1 mmol) of neocuproine hydrate in a volume of 100 mL of aqueous methanol (20 volume % MeOH). Silica gel (1.00 g), weighed at ambient temperature and humidity, was added to 10–15 flasks for each of three data sets using Merck 10181, Davisil 643, and Merck 9385 silicas. Aliquots of 2 mL of 0.1 M HCl and 2 mL of 1 M sodium nitrate were added to each flask followed by 8 mL of $[\text{Co}(\text{neo})]^{2+}$ stock. The pH was increased incrementally from one flask to the next within the range 2.5–9.6 by addition of triethylamine in 10 vol % aqueous methanol contributing a total volume of 10 mL to each flask. The final concentrations were 0.009 M HCl, 0.09 M NaNO_3 , and 0.0036 M $[\text{Co}(\text{neo})(\text{solvent})_4]^{2+}$. The solvent composition was less than 12 vol % MeOH for all samples. The pH of the supernatant was measured after the flasks were incubated overnight at a temperature of 25 °C. The concentration of cobalt was determined as already described. Two important working assumptions for the accuracy of pH measurements were made: (1) The presence of up to 12% methanol would have little effect on the pH readings relative to aqueous solution,¹⁷ and (2) the effects of potential differences (Z) between the surface of the silica and the supernatant could be treated as negligible, as demonstrated by Schindler and co-workers for a similar system.¹⁸

D. Isotherm Data. A series of stock solutions including a 0.10 M aqueous solution of HCl, a 0.2 M solution of Et_3N in aqueous methanol (10 volume % MeOH), and a 1 M aqueous solution of NaNO_3 were prepared and added in aliquots of 2, 2.5, and 4 mL, respectively, to 12 flasks each containing 1.00 g of silica gel. A 0.01 M stock solution (20% volume MeOH) of $[\text{Co}(\text{neo})]^{2+}$ was added to each of the 12 flasks with a final concentration ranging from 0.2 to 6.5 mM. The overall volume was kept constant at 24.5 mL for each sample by the addition of a 20% vol MeOH solution when necessary. The pH of each solution was 8.5 ± 0.5 . After incubation at 25 °C for 24 h, the amount of bound cobalt was determined using either method 1 or 2 (vide supra), depending on the relative amounts of adsorbed and unbound $\text{Co}(\text{II})$. Langmuir analyses were performed by determining Γ_{pH} (the number of moles of adsorbate bound per square meter of material, measured at constant pH)^{19,20} and plotting these data as a function of the equilibrium concentration of unbound cobalt concentration in solution.

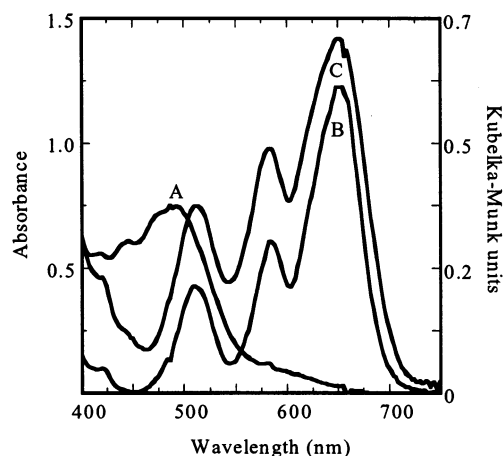


Figure 1. Spectra of solution and silica-supported $[\text{Co}(\text{neo})]^{2+}$: (A) 0.050 M $[\text{Co}(\text{neo})]^{2+}$ solution spectrum; (B) 0.005 M $[\text{Co}(\text{neo})]^{2+}$ in a transparent silica sol–gel with $[\text{OH}^-]/[\text{Co}^{2+}] = 2$. (C) Diffuse reflectance spectrum of $6.7 \times 10^{-6} \text{ mol g}^{-1}$ $[\text{Co}(\text{neo})]^{2+}$ bound to M480 silica (Table 2).

IV. Adsorption on Sol–Gel Silicas. A. Sol–gel Synthesis.

Silica sol was prepared by mixing 7.5 mL of deionized H_2O (0.860 mol), 15.5 mL (0.104 mol) of distilled tetramethyl orthosilicate (Acros), and 0.1 mL of 0.1 M HCl (10 μmol) and sonicating the mixture for 10 min. The initially biphasic mixture afforded a clear, colorless sol, which was used in the following experiments without further manipulation.

B. Titration of $[\text{Co}(\text{neo})]^{2+}$ in Sol–Gel with Base. A 0.1 M stock solution of $[\text{Co}(\text{neo})]^{2+}$ was prepared from 2.91 g of $[\text{Co}(\text{NO}_3)_2 \cdot 6\text{H}_2\text{O}]$ (J. T. Baker) and 2.08 g of neocuproine hydrate (GFS) in a volume of 100 mL of MeOH. Three dilutions were made from this stock solution, affording stocks with concentrations of 0.05, 0.025, and 0.02 M, diluted appropriately to maintain a constant 50:50 vol/vol ratio of MeOH/ H_2O . A volume of 0.7 mL of $[\text{Co}(\text{neo})]^{2+}$ was added to each of 28 cuvettes, in 4 sets of 7, with each set of 7 samples representing one of the cobalt stock concentrations. Sonicated sol (2.3 mL) was then added to each of the 28 cuvettes. NaOH (1 M) was then added to each cuvette to achieve different values of the ratio $[\text{OH}^-]/[\text{Co}^{2+}]$ in the range 0–2.5. To determine the maximal loading of $[\text{Co}(\text{neo})]^{2+}$ within the sol–gel material, the amount of sonicated sol was reduced to 1.5, 0.5, or 0.25 mL, and solutions of 0.1 M $[\text{Co}(\text{neo})]^{2+}$ in methanol were increased to 1, 2.0, or 2.25 mL, respectively. Addition of NaOH consisted of a volume of 0.5 or 0.56 mL of the appropriate concentration of NaOH to obtain $[\text{OH}^-]/[\text{Co}^{2+}] = 2$.

Results and Discussion

I. Binding of Cobalt Neocuproine to Silica Gel. A.

$[\text{Co}(\text{neo})(\text{solvent})_4]^{2+}$ ($[\text{Co}(\text{neo})]^{2+}$). A 1:1 mixture of $[\text{Co}(\text{NO}_3)_2 \cdot 6\text{H}_2\text{O}]$ and neocuproine (2,9-dimethyl-1,10-phenanthroline) in aqueous methanol solutions afforded an orange-pink complex of low color intensity ($\lambda_{\text{max}} = 486 \text{ nm}$, $\epsilon = 15 \text{ M}^{-1} \text{ cm}^{-1}$) typical of an octahedral species, assumed to be $[\text{Co}(\text{neo})(\text{solvent})_4]^{2+}$ (Figure 1, curve A). The compound gave needlelike crystals on evaporation of methanol–water solutions, but attempts to obtain the X-ray structure of the complex were unsuccessful because of difficulties in obtaining a reasonable unit cell based on their diffraction patterns. However, as will be discussed in section B.2, the XANES spectrum of $[\text{Co}(\text{neo})(\text{solvent})_4]^{2+}$ shows a weak

(17) Bosch, E.; Bou, P.; Allemann, H.; Roses, M. *Anal. Chem.* **1996**, *68*, 3651–3657.

(18) Schindler, P. W.; Furst, B.; Dick, R.; Wolf, P. U. *J. Colloid Interface Sci.* **1976**, *55*, 469–475.

(19) Vordonis, L.; Spanos, N.; Koutsoukos, P. G.; Lycourghiotis, A. *Langmuir* **1992**, *8*, 1736–1743.

(20) Stumm, W.; Morgan, J. J. In *Aquatic Chemistry*, 3rd ed.; Schnoor, J. L., Zehnder, A., Eds.; John Wiley & Sons: New York, 1996; pp 521–523.

pre-edge feature assigned to a $\text{Co } 1s \rightarrow 3d$ transition that is consistent with a six-coordinate geometry.²¹

B. Surface Binding of $[\text{Co}(\text{neo})]^{2+}$: Structure of the Bound Complex. 1. Visible and Vibrational Spectroscopy.

When aqueous methanol solutions of $[\text{Co}(\text{neo})]^{2+}$ were mixed with silica gel, an intensely blue species formed on the silica surface (Figure 1, curve B). The adsorption was very rapid, and the color change strongly suggested a change in coordination number at the cobalt center.²² The diffuse reflectance visible spectrum of this surface-bound complex, $[\text{Co}(\text{neo})(\text{silica})]^{n+}$, exhibited three distinct maxima, at 654, 584, and 512 nm. Intensities for these spectral features were not directly comparable to those obtained for the six-coordinate precursor in solution; spectra obtained in transparent sol-gel materials, $[\text{Co}(\text{neo})(\text{sol-gel})]^{n+}$ (vide infra), however, had $\epsilon = 245, 121, \text{ and } 86 \text{ M}^{-1} \text{ cm}^{-1}$, respectively, consistent with a change in coordination upon binding.²²

For tetrahedral $\text{Co}(\text{II})$ complexes, the absorbances observed in the visible region correspond to the high energy (${}^4\text{T}_1(\text{P}) \leftarrow {}^4\text{A}_2$) electronic transition, with the lower energy ν_2 (${}^4\text{T}_1(\text{F}) \leftarrow {}^4\text{A}_2$) and ν_1 (${}^4\text{T}_2 \leftarrow {}^4\text{A}_2$) transitions occurring in the near-IR and IR regions, respectively.^{23,24} When the symmetry of a tetrahedral compound is lowered to C_{2v} , the orbital triplet level, T_1 , splits into three energy levels, producing the two additional peaks in the spectrum.^{23,25} The degree of splitting (lowest to highest energy peak energy separation within ν_3) in the visible transition has been interpreted as arising from a high degree of distortion from an idealized tetrahedral structure.²³ Three distinct peaks with a large degree of splitting in the visible region have been observed in the spectrum of the distorted pseudotetrahedral 2N,2O-bound cobalt adduct, $[\text{KCo}(\text{neo})(\text{XDK})(\text{PF}_6)]$ (Figure 2, peaks in the visible at 646, 566, and 496 nm)²⁶ and in the spectrum of the Co^{2+} center in cobalt silicate (peaks in the visible at 645, 595, and 525 nm).^{27,28} The degree of splitting of ν_3 in the $[\text{Co}(\text{neo})]^{2+}$ surface complex, 132 nm, was greater than that of cobalt silicate, 120 nm, and less than that of the XDK adduct, 150 nm.

Because X-ray crystallographic data are necessarily unavailable for cobalt silicate, a more tangible evaluation of the relationship between splitting of ν_3 and the metal ion coordination environments can be made using crystallographically characterized $[\text{KCo}(\text{neo})(\text{XDK})(\text{PF}_6)]^{26}$ and

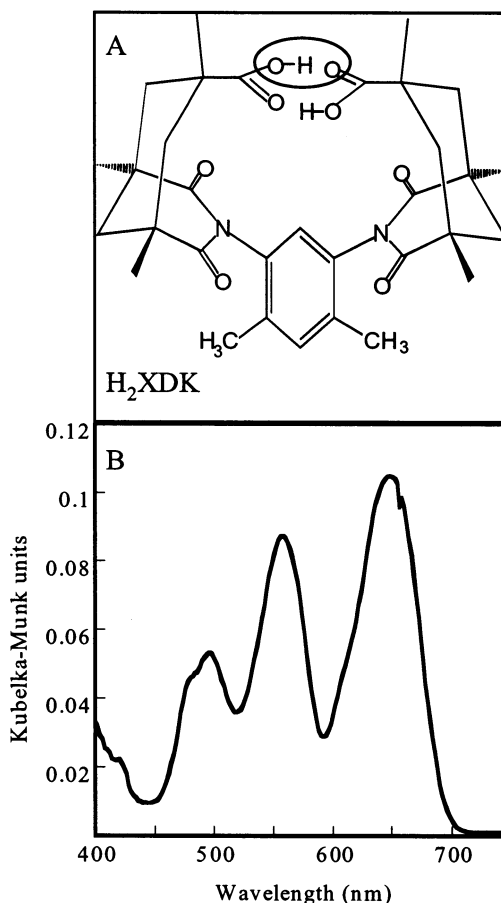


Figure 2. Diffuse reflectance spectra of $[\text{KCo}(\text{neo})(\text{XDK})(\text{PF}_6)]$ (B) whose synthesis and characterization has been previously described in ref 26 and the structure of H_2XDK , xylenediamine bis(Kemp's triacid imide) with the oxygen atoms that bind to $\text{Co}(\text{II})$ circled (A).

$[\text{Co}(\text{neo})\text{X}_2]^{29}$ ($\text{X} = \text{Br}^-$ and SCN^- prepared for comparative purposes, Supporting Information). The Br^- and SCN^- adducts showed either very similar, or crystallographically identical,²⁹ $\text{Co}-\text{X}$ bond distances; although the electronic spectra for these adducts were similar to that of the surface species, they did not exhibit the extensive splitting observed in the visible region for the XDK complex, cobalt silicate, or the surface-bound $[\text{Co}(\text{neo})]^{2+}$ complex. The $[\text{Co}(\text{neo})]^{2+}$ structural unit was found to be essentially invariant between the XDK and $[\text{Co}(\text{neo})\text{X}_2]$ structures; it thus appears that the most important contribution to the apparent symmetry-lowering in the electronic structure of $[\text{Co}(\text{neo})(\text{silica})]^{n+}$ and $[\text{KCo}(\text{neo})(\text{XDK})(\text{PF}_6)]$ is the asymmetry about the other bonds to the cobalt ion. We conclude, on the basis of the strong resemblance of the spectra of the complexes, that the $[\text{Co}(\text{neo})(\text{silica})]^{n+}$ adduct is most likely distorted from T_d to a comparable extent as is observed in $[\text{KCo}(\text{neo})(\text{XDK})(\text{PF}_6)]$.

The IR spectra for the surface-bound $[\text{Co}(\text{neo})]^{2+}$ compound were difficult to obtain because of the silica background. However, several peaks were detectable below 1700 cm^{-1} , in the regions associated with ring stretching and out-of-plane bending for bonds of the neocuproine ligand.

- (21) Wirt, M. D.; Sagi, I.; Chen, E.; Frisbie, S. M.; Lee, R.; Chance, M. R. *J. Am. Chem. Soc.* **1991**, *113*, 5299–5304.
 (22) McMillin, D. R.; Rosenberg, R. C.; Gray, H. B. *Proc. Natl. Acad. Sci. U.S.A.* **1974**, *71*, 4760–4762.
 (23) Goodgame, D. M. L.; Goodgame, M. *Inorg. Chem.* **1965**, *4*, 139–143.
 (24) Peaks found for $[\text{Co}(\text{neo})(\text{sol-gel})]^{n+}$ were the following: 10230(sh), 8382, and 6569 cm^{-1} (ν_2 region); $\sim 4400 \text{ cm}^{-1}$ (ν_1 region). Assignments were based on comparisons of the $[\text{Co}(\text{neo})\text{X}_2]$ compounds with their corresponding zinc analogues.
 (25) Tomlinson, A. A. G.; Bellitto, C.; Piovesana, O.; Furlani, C. *J. Chem. Soc., Dalton Trans.* **1971**, 350–354.
 (26) Watton, S. P.; Davis, M. I.; Pence, L. E.; Rebek, J., Jr.; Lippard, S. J. *Inorg. Chim. Acta* **1995**, *235*, 195–204.
 (27) Reisfeld, R.; Jorgensen, C. K. In *Coordination Chemistry*; American Chemical Society: Washington, DC, 1994; Vol. 565, pp 439–443.
 (28) Reisfeld, R.; Jorgensen, C. K. *Struct. Bonding (Berlin)* **1992**, *77*, 207–265.

(29) Taylor, C. M.; Watton, S. P.; Pence, L. Unpublished results, 2002.

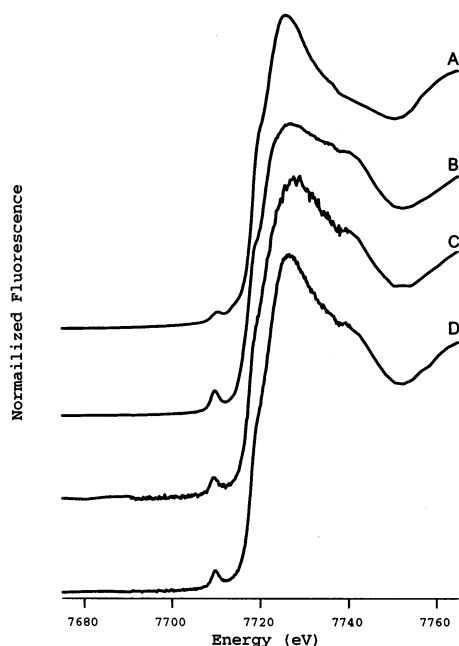


Figure 3. Co K-edge XANES for compounds A–D. Edge energies and 1s–3d peak areas are listed in Table 1. The compounds are as follows: **A**, $[\text{Co}(\text{neo})(\text{H}_2\text{O})_4](\text{NO}_3)_2$; **B**, $[\text{KCo}(\text{neo})(\text{XDK})(\text{PF}_6)]$; **C**, $[\text{Co}(\text{neo})(\text{silica})]^{n+}$; and **D**, $[\text{Co}(\text{neo})(\text{sol-gel})]^{n+}$.

Primarily, the presence of these peaks confirms the presence of the neocuproine ligand in the surface-bound complex. Minor shifts in these peaks were observed for the surface adduct when compared to the free ligand and were consistent with the $[\text{Co}(\text{neo})\text{X}_2]$ compounds (Table S5 Supporting Information). Such minor shifts in the vibrational spectroscopy are apparent upon coordination of phenanthroline compounds to a variety of metals.³⁰

2. X-ray Spectroscopy. X-ray absorption spectra, particularly the K-edge XANES spectra (Figure 3), for the surface-adsorbed species provide support for the partial structural assignment inferred from the electronic spectra. Four complexes were examined, including the pseudo-octahedral precursor complex $[\text{Co}(\text{neo})(\text{solvent})_4](\text{NO}_3)_2$, $[\text{KCo}(\text{neo})(\text{XDK})(\text{PF}_6)]$ as the surface complex structural model, and two samples of the $[\text{Co}(\text{neo})]^{2+}$ surface complexes, $[\text{Co}(\text{neo})(\text{silica})]^{n+}$, which was synthesized by grafting to Merck 9385 silica, and $[\text{Co}(\text{neo})(\text{sol-gel})]^{n+}$ using sol-gel processing.

The Co K-edge XANES spectra obtained for $[\text{Co}(\text{neo})(\text{H}_2\text{O})_4](\text{NO}_3)_2$, $[\text{KCo}(\text{neo})(\text{XDK})(\text{PF}_6)]$, $[\text{Co}(\text{neo})(\text{silica})]^{n+}$, and $[\text{Co}(\text{neo})(\text{sol-gel})]^{n+}$ are compared in Figure 3 and Table 1. The Co K-edge energies observed for the samples fall into a narrow range from 7717.8 to 7718.4 eV, consistent with all samples containing Co(II) ions in similar ligand environments.³¹ In each case, a pre-edge peak that can be assigned to a Co 1s \rightarrow 3d transition was observed between 7709 and 7711 eV.²¹ The intensity of this feature is directly related to the extent of Co p–d orbital mixing and is therefore

expected to be small for centrosymmetric ligand geometries and larger for noncentrosymmetric geometries.^{21,31,32}

The largest pre-edge peak area (15.7×10^{-2} eV) is observed for $[\text{KCo}(\text{neo})(\text{XDK})(\text{PF}_6)]$, whose crystal structure shows it to feature Co in a distorted tetrahedral ligand arrangement.²⁶ The smallest peak area (4.8×10^{-2} eV) is observed for $[\text{Co}(\text{neo})(\text{H}_2\text{O})_4](\text{NO}_3)_2$ and is consistent with a more centrosymmetric six-coordinate geometry. The XANES spectra obtained for $[\text{Co}(\text{neo})(\text{silica})]^{n+}$ and $[\text{Co}(\text{neo})(\text{sol-gel})]^{n+}$ complexes are essentially identical, indicating that the same complex is present in both materials. The area obtained for the pre-edge peak for the supported $[\text{Co}(\text{neo})]^{2+}$ complexes is also within experimental error for both materials and is large, but not as large as that observed for $[\text{KCo}(\text{neo})(\text{XDK})(\text{PF}_6)]$, and is therefore consistent with a distorted tetrahedral or five-coordinate geometry for the Co center. The XANES spectrum obtained for $[\text{KCo}(\text{neo})(\text{XDK})(\text{PF}_6)]$ is quite similar, but not identical to those obtained from the supported $[\text{Co}(\text{neo})]^{2+}$ samples. In general, $[\text{KCo}(\text{neo})(\text{XDK})(\text{PF}_6)]$ appears to be a good structural model for the supported complexes.

The number of ligand donor atoms in the primary coordination sphere of Co is difficult to determine from analysis of EXAFS. This is because of the presence of both O- and N-donor atoms at similar but nonidentical distances, which gives rise to a high degree of static disorder in the Co–L distances. As a result, four well-ordered Co–O/N distances can give as similar an EXAFS amplitude as six less well-ordered Co–O/N distances. This correlation effectively limits the accuracy of the determination of the number of scattering atoms (*N*) in a refined shell to ca. $\pm 25\%$ or ± 1 donor atom. For this reason, the XANES data discussed here are a more reliable indicator of coordination number and geometry, and the EXAFS data will be discussed only briefly with more detail in Supporting Information (Figure S1, Tables S3–S7).

Overall, the EXAFS spectra for the supported $[\text{Co}(\text{neo})]^{2+}$ complexes are very similar to that obtained for $[\text{KCo}(\text{neo})(\text{XDK})(\text{PF}_6)]$, and distinct from the EXAFS spectrum obtained from $[\text{Co}(\text{neo})(\text{H}_2\text{O})_4](\text{NO}_3)_2$, in accord with the results of the XANES analysis. Consistent with the expected higher coordination number, the average Co–N distance obtained from the single shell fit for $[\text{Co}(\text{neo})(\text{H}_2\text{O})_4](\text{NO}_3)_2$ (2.12(2) Å) is significantly longer than the distances obtained from the other samples (2.00(2) Å), which are identical within experimental error. The average O/N distance for $[\text{KCo}(\text{neo})(\text{XDK})(\text{PF}_6)]$ obtained from the EXAFS analysis (2.00(2) Å) agrees well with the average of the two Co–N and two Co–O bonds in the crystal structure (2.007(68) Å).²⁶ This result supports the conclusion from XANES analysis that the structure of $[\text{KCo}(\text{neo})(\text{XDK})(\text{PF}_6)]$ is quite similar to those of the supported $[\text{Co}(\text{neo})]^{2+}$ complexes and distinct from $[\text{Co}(\text{neo})(\text{H}_2\text{O})_4](\text{NO}_3)_2$.

C. pH Dependence. To better determine the chemical nature of the supported adduct, and to gain some insight into

(30) Schilt, A. A.; Taylor, R. C. *J. Inorg. Nucl. Chem.* **1959**, *9*, 211–221.

(31) Colpas, G. J.; Maroney, M. J.; Bagyinka, C.; Kumar, M.; Willis, S. W.; Suib, S. L.; Mascharak, P. K.; Baidya, N. *Inorg. Chem.* **1991**, *30*, 920–928.

(32) Roe, A. L.; Schneider, D. J.; Mayer, R. J.; Pyrz, J. W.; Widom, J.; Que, L., Jr. *J. Am. Chem. Soc.* **1984**, *106*, 1676–1681.

Table 2. Silica Samples Used for pH Dependence on Adsorption and Langmuir Analysis

manufacturer	grade	SA ($\text{m}^2 \text{g}^{-1}$)	pore diam \AA	$\Gamma_{(\text{pH}8)\text{max}}^a$ (mol m^{-2}) $\times 10^7$	approx loading ^b	
M675	Merck	10181	675	40	3.4	6
M480	Merck	9385	480	60	5.9	7
D300	Davisil	643	300	150	8.9	7

^a Results of the Langmuir analysis (section E) obtained by nonlinear fits to eq 6. ^b $[\text{Co}(\text{neo})]^{2+}/[\text{Si}] \times 10^4$.

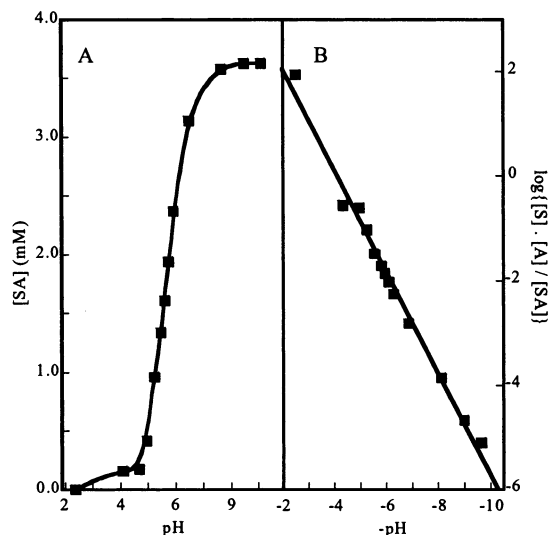
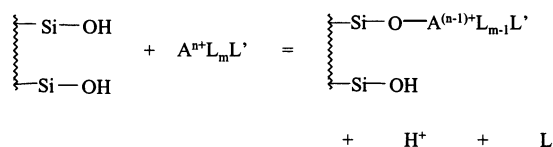


Figure 4. pH dependence of surface binding. Titration data indicating amount of $[\text{Co}(\text{neo})]^{2+}$ bound to M480 silica as a function of solution pH (A). Linearized data from (A) for M480 silica (B). Slope indicates the number of protons released per $[\text{Co}(\text{neo})]^{2+}$ bound.

the generality of the exchange reaction, we examined the pH dependence of $[\text{Co}(\text{neo})]^{2+}$ binding on silica surfaces, for three silica samples having a range of surface areas and average pore diameters (Table 2).

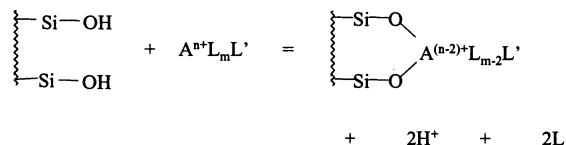
For simplicity, we will refer to these samples as M675, M480, and D300, M and D referring to the manufacturers Merck and Davisil, respectively, and the numerical values referring to the BET surface area³³ of each sample in grams per square meter. The concentration of $[\text{Co}(\text{neo})]^{2+}$ adsorbed on the surface was determined at each pH value for separate samples as described in the Experimental Section. The molarities of the $[\text{Co}(\text{neo})]^{2+}$ adsorbate solutions were chosen to ensure that the measurements were made under subsaturation conditions, although the measurements made on the M675 sample were later found to be closer to saturation than expected (Figure S2, Supporting Information). Appropriate concentrations were determined by Langmuir analysis, as detailed in a following section. Formation of the blue surface species was observed at or above pH 5 with maximal binding around pH 8 for all samples (Figure 4A, M480 shown). At $\text{pH} \geq 8$, over 95% of the cobalt neocuproine in solution became bound to silica samples M480 and D300. Formation of cobalt hydroxide species in the adsorbate solution for sample M675 above pH 8

Mode 1



$$K = \frac{\{(\text{SiOA})\}[\text{H}^+]}{\{(\text{SiOH})\}\{\text{A}\}}$$

Mode 2



$$\beta = \frac{\{(\text{SiO})_2\text{A}\}[\text{H}^+]^2}{\{(\text{SiOH})_2\}\{\text{A}\}}$$

Figure 5. Possible binding modes for $[\text{Co}(\text{neo})]^{2+}$ on the silica surface based on a monodentate (1) and bidentate (2) interaction. Below each binding mode is the appropriate equilibrium expression where A = Co^{2+} (adsorbate) in solution and SiOA or $(\text{SiO})_2\text{A}$ = Co^{2+} bound to the surface. L is an exchangeable ligand such as water (in aqueous solution activity is 1). L' is a nonexchangeable bidentate ligand such as neocuproine. Adapted from ref 20.

prevented a confident determination of concentration at higher pH values.

In accord with binding studies of similar compounds,^{2,5,34,35} two equilibrium expressions can be written for the binding event (Figure 5). The binding at the surface based on mode 1 is doubly proton-dependent, whereas that based on 2 is singly proton-dependent. To determine the proton dependence of the reaction between $[\text{Co}(\text{neo})]^{2+}$ and silica gel, the pH data were linearized by plotting the logarithm of the singly and doubly proton-dependent equilibrium expressions (eqs 1a and 2a):

$$\log\{[\text{SiOH}][\text{A}]/[\text{SiOA}]\} = -\log K_{\text{Co}} - \text{pH} \quad (1a)$$

$$([\text{SiOH}]_{\text{T}} - [\text{SiOA}]) = [\text{SiOH}] \quad (1b)$$

$$\log\{[(\text{SiOH})_2][\text{A}]/[(\text{SiO})_2\text{A}]\} = -\log K_{\text{Co}} - 2\text{pH} \quad (2)$$

$$((\text{SiOH})_2)_{\text{T}} - [(\text{SiO})_2\text{A}] = [(\text{SiOH})_2] \quad (2b)$$

The total number of surface sites equals the maximal binding of surface species, as derived from the Langmuir isotherm data (section D). The equilibrium concentration of surface sites is obtained by subtraction of the equilibrium concentration of the bound cobalt neocuproine from the total number of surface sites according to mass laws (eqs 1b and 2b). Activities were assumed equal to concentration under the experimental conditions ($[\text{NaNO}_3] \sim 0.1 \text{ M}$). When the linear expression is used to plot the experimental data, a slope of 1 would indicate $[\text{Co}(\text{neo})(\text{SiO})(\text{H}_2\text{O})]^+$ as the most likely surface species. A slope of 2 would indicate a bidentate

(33) Brunauer, S.; Emmett, P. H.; Teller, E. G. *J. Am. Chem. Soc.* **1938**, *60*, 309–317.

(34) Badieli, A.-R.; Bonneviot, L. *Inorg. Chem.* **1998**, *37*, 4142–4145.

(35) Burland, D. M.; Miller, R. D.; Walsh, C. A. *Chem. Rev.* **1994**, *94*, 31–75.

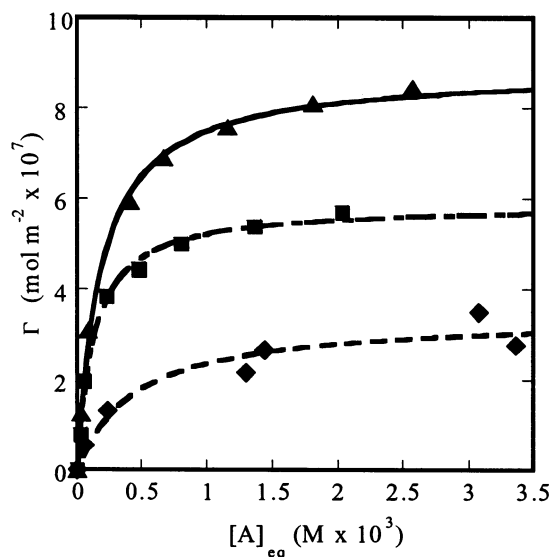


Figure 6. Langmuir binding data for commercial silica gels. Lines represent nonlinear fits to the Langmuir expression $\Gamma_{\text{pH8}} = \Gamma_{(\text{pH8})\text{max}} \cdot \{K_{\text{ads}} \cdot [\text{A}] / (1 + K_{\text{ads}} \cdot [\text{A}])\}$, where $[\text{A}]$ is the equilibrium concentration of Co^{2+} in solution. Key: D300, \blacktriangle ; M480, \blacksquare ; M675, \blacklozenge (Table 2).

silanol mode of binding forming $[\text{Co}(\text{neo})(\text{SiO})_2]$ with concomitant loss of two protons from the silica surface.

The slopes for the linear plot according to eqs 1a and 2a for all three silica gels fall slightly under a value of 1 (0.972–0.834) with correlation factors > 0.99 (Figure 4B, linear fit to data for silica M480 shown). Given the simplifications made in describing the chemistry of the adsorption event, and the assumption of negligible potential difference between the surface and solution for pH measurements,¹⁸ the fits are sufficiently good to infer a singly proton-dependent equilibrium. These results are entirely consistent with the formulation of $[\text{Co}(\text{neo})(\text{SiO})(\text{H}_2\text{O})]^+$ for the surface-bound species, as described.

D. Isotherm Data. Langmuir analyses according to eq 3 were used to evaluate the potential maximal binding of $[\text{Co}(\text{neo})]^{2+}$ per square meter of material ($\Gamma_{(\text{pH})\text{max}}$) to the surfaces of three commercial silica gel samples M675, M450, and D300 (Table 2, Figure 6).

$$\Gamma_{\text{pH}} = \Gamma_{(\text{pH})\text{max}} \times \{K_{\text{ads}} \times [\text{A}] / (1 + K_{\text{ads}}[\text{A}])\} \quad (3)$$

$\Gamma_{(\text{pH})\text{max}}$ values for the three samples were inversely proportional to surface area and proportional to pore size with values of 3.4 , 5.9 , and 8.9×10^{-7} mol m^{-2} for samples M675, M450, and D300, respectively. A comparison was also made between two commercial silica samples D300 ($\text{SA} = 300$ m^2 g^{-1} , pore diameter 150 Å) and Merck 10184, M300, ($\text{SA} = 300$ m^2 g^{-1} , pore diameter 100 Å) with the same reported surface area but different pore size. The M300 silica sample bound 10% less $[\text{Co}(\text{neo})]^{2+}$ than the D300 sample; 8.1×10^{-7} compared to 8.9×10^{-7} , respectively (data not shown). These data indicated that the primary factor in determining maximal loading was the contribution of pore size to the total reported surface area. Fits to Langmuir data were also evaluated for a secondary adsorbed species or a second adsorption site of lower affinity. Although good fits

using these models were obtained (data not shown), the resultant parameters obtained for a second K_{ads} for an additional adsorbed species were less than 10^{-9} . When compared to the values obtained for binding of a single species (range = $2\text{--}8 \times 10^{-3}$), these values were considered insignificant and support the contention that a single type of surface adduct is formed. An excellent Beer's law correlation between the transmittance values obtained from reflectance spectra (expressed in Kubelka–Munk units) as a function of the measured Co(II) loadings for several 1 g silica samples (Figure S4) provided further evidence for homogeneity of the surface species.

II. Cobalt Neocuproine Doped in Sol–Gel. A. Comparison of $[\text{Co}(\text{neo})]^{2+}$ in Solution and in Sol–Gel. The clear spectral changes that occur on binding of $[\text{Co}(\text{neo})]^{2+}$ to silica surfaces make the chemistry a potentially useful probe for the coordination chemistry associated with grafting of metal complexes during sol–gel reactions. We were particularly interested in how the structural chemistry of the surface binding reaction might be affected by the sol–gel conditions, and whether the sol–gel approach could be used to afford significantly higher loadings of metal complexes while maintaining comparable site homogeneity.

Tetramethyl orthosilicate (TMOS) sol–gels were prepared using an acid-catalyzed procedure ($[\text{H}^+] = 0.2$ mM). Consistent with the pH dependence of the $[\text{Co}(\text{neo})]^{2+}$ binding to the surfaces of commercial silica gels, the octahedral complex did not exhibit reactivity with the silica gel without the addition of base. Addition of $[\text{Co}(\text{neo})\text{-(solvent)}_4]^{2+}$ to the sols afforded an orange mixture, with the same spectrum, λ_{max} at 486 nm ($\epsilon = 15$ M^{-1} cm^{-1}), as that observed for the octahedral species in aqueous methanol solution (50:50 vol/vol). The similarity in the spectroscopic characteristics of the octahedral complex in solution and in sol allowed for the determination of the molar absorptivity increase that accompanied the formation of the tetrahedral surface complex.

B. Formation of $[\text{Co}(\text{neo})(\text{sol-gel})]^{2+}$. Addition of base to the $[\text{Co}(\text{neo})]^{2+}$ -doped sol caused the appearance of the blue color characteristic of the surface-bound species. The three distinct maxima in the visible spectrum of the sol–gel species were identical to those observed in the reflectance spectrum of the silica-bound species (Figure 1, curves B and C). Because optically transparent monoliths containing the blue surface-bound species could be produced, it was possible to measure a transmission extinction coefficient for the tetrahedral adduct. The molar absorptivity of the surface species at each λ_{max} was roughly 16 times that of the octahedral species at 245 M^{-1} cm^{-1} , under conditions where the concentration of base was sufficient to ensure essentially quantitative conversion to the surface species (vide infra). Such a change in extinction coefficient is consistent with a decrease in coordination number from six to four or five.²²

Direct measurement of pH by a glass electrode is not possible for the viscous sol during the sol–gel process without destruction of the electrode or erroneous readings. However, an estimate of the concentration of hydroxide per cobalt center, $[\text{OH}^-]/[\text{Co}^{2+}]$, was obtained using the initial

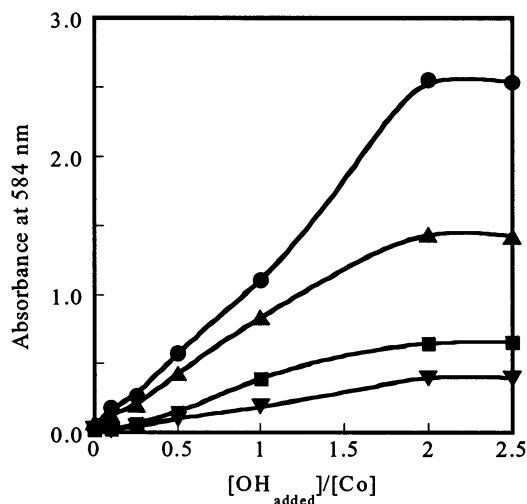


Figure 7. NaOH titration for sol–gels containing $[\text{Co}(\text{neo})]^{2+}$ at concentrations, from top to bottom, 21.9, 11.3, 5.6, and 3.3 mM. Absorbance values were not taken at 654 nm because of the intensity of the sample at 21.9 mM. The lines are smooth fits to the data points to aid the eye and do not represent a fit to a specific equation.

amount of acid catalyst subtracted from the amount of NaOH added to the post-sonicated solution. In contrast to the results with commercial silica gels, titration of $[\text{Co}(\text{neo})]^{2+}$ with base in silica sol showed maximal absorption intensity of the tetrahedral adduct at approximately 2 equiv of added base per cobalt at four different concentrations of $[\text{Co}(\text{neo})]^{2+}$ (Figure 7). There were no spectroscopic differences, with the exception of intensities, between gels having 1 equiv of added base versus those containing 2 equiv, suggesting a cooperative two-proton-dependent binding event. The maximum loading of $[\text{Co}]/[\text{Si}]$ obtained while still maintaining gel transparency after addition of 2 equiv of hydroxide anion was 1.22×10^{-3} , corresponding to a 2-fold increase in loading over surface grafting. Maximal loadings for opaque silica gels as high as 27-fold over surface grafting were obtained; we did not attempt to obtain higher loadings.

The similarity of the visible and XAS spectra (section I.B) for the sol–gel and impregnated silica samples indicate very similar coordination environments for $[\text{Co}(\text{neo})]^{2+}$ bound to either material which seems to contrast with the pH-dependence data. This apparent discrepancy is noted but at present has not been satisfactorily resolved.

Summary

Taken together, the data presented here provide a clear and self-consistent picture of the ICC reactivity of the $[\text{Co}(\text{neo})]^{2+}$ fragment. On the basis of electronic and X-ray absorption data, it is evident that the surface binding reaction is accompanied by a significant change in coordination geometry at the cobalt centers, regardless of whether the complexes are grafted onto a preformed silica or incorporated at the inception of silica formation by sol–gel processing. The XAS data demonstrate a striking similarity between the structurally characterized XDK compound and the new surface species, indicating a highly distorted four-coordinate environment about the Co(II) center. Changes in the geom-

etry at cobalt are probably driven by steric interactions between the 2,9-dimethyl substituents on neocuproine and the silica surface. Evidence for steric influences on surface binding have been observed previously, such as the preference for the $[\text{Co}(\text{en})_2]^{3+}$ fragment to bind to silica in the cis configuration, which contrasts with the solution preference for the trans configuration.³⁶

Binding to the silica surface appears to involve coordination to Co^{2+} by at least one inner-sphere silanolate ligand. The requirement of 2 equiv of hydroxide for maximal surface-binding in the sol–gel environment appeared to indicate a doubly proton-binding event. Despite the different dependence on hydroxide concentration, no significant differences in the binding modes could be detected by visible or XAS spectroscopies. The spectral resolution of the visible data may not be sufficient to differentiate between $[\text{Co}(\text{neo})\text{-(SiO)}(\text{H}_2\text{O})]^+$ and $[\text{Co}(\text{neo})(\text{SiO})_2]$, however, because the ligand field strengths of SiO^- and H_2O have been shown to be very similar.⁵

The isotherm data indicated that the highest surface coverage was attained using the silica sample D300 with the lowest surface area but largest pore diameter. The presence of larger pores suggests a flatter terrain at the surface that would be less likely to hinder adsorption because of steric reasons, whereas the silica gels having smaller pores reduce the available surface area by steric occlusion. Loading of $[\text{Co}(\text{neo})]^{2+}$ on the silica samples is roughly similar between samples (Table 2) while significantly higher loading of the surface species, at least 27-fold relative to the commercial silica (Table 2), could be attained by the sol–gel methods. A transparent sol–gel material could be produced with twice the loading of $[\text{Co}(\text{neo})]^{2+}$ despite the need of base to activate the surface groups which typically collapses the silica structure.¹ The extent of loading does not, however, always indicate that all dopant molecule are accessible to take part in further reactions.³⁷ This phenomenon was demonstrated by the incomplete reaction of the $[\text{Co}(\text{neo})]^{2+}$ centers in dried sol–gel samples on treatment with 1 M HCl.

On the basis of the results presented here, substitution-labile $[\text{Co}(\text{phen})]^{2+}$ complexes have excellent characteristics for use as probes of steric interactions between metal complexes and the silica surface: interfacial equilibria are attained rapidly because of the substitution-labile nature of the high-spin d^7 metal ion, and surface binding is accompanied by readily detectable spectroscopic changes, which can be monitored most conveniently in transparent sol–gel materials. Work is in progress to determine the effects of changing steric bulk around the cobalt center on the formation and structure of the surface adducts, and in turn how these structural features might affect their catalytic behavior.

Acknowledgment. We thank the Thomas and Kate Miller Jeffress Memorial Trust and the Research Corporation for

(36) Beland, F.; Badiei, A. R.; Ronning, M.; Nicholson, D.; Bonneviot, L. *Phys. Chem. Chem. Phys.* **1999**, *1*, 605–613.

(37) Dunn, B.; Zink, J. I. *Chem. Mater.* **1997**, *9*, 2280–2291.

funding. Dr. Stephen P. Watton is a Cottrell Scholar of the Research Corporation. The National Light Source (NSLS) at Brookhaven National Laboratory is supported by the U.S. Department of Energy, Division of Materials Sciences and Division of Chemical Sciences. Beamline X9B at NSLS is supported in part by NIH Grant RR-01633. We thank Dr. Laura E. Pence, University of Hartford, for providing crystal

structure data for $[\text{Co}(\text{neo})(\text{SCN})_2]$ and $[\text{Co}(\text{neo})\text{Br}_2]$ and Dr. F. M. Hawkrige for helpful comments on the manuscript.

Supporting Information Available: Synthesis and characterization data. This material is available free of charge via the Internet at <http://pubs.acs.org>.

IC025824R